View metadata, citation and similar papers at core.ac.uk

brought to you by CORE

provided by JRC Publications Repository

JRC Scientific and Technical Reports

ANALYSIS OF TOXICITY EFFECTS FROM MOLECULAR TO POPULATION LEVEL: Circadian oscillator case study

José-Manuel Zaldívar

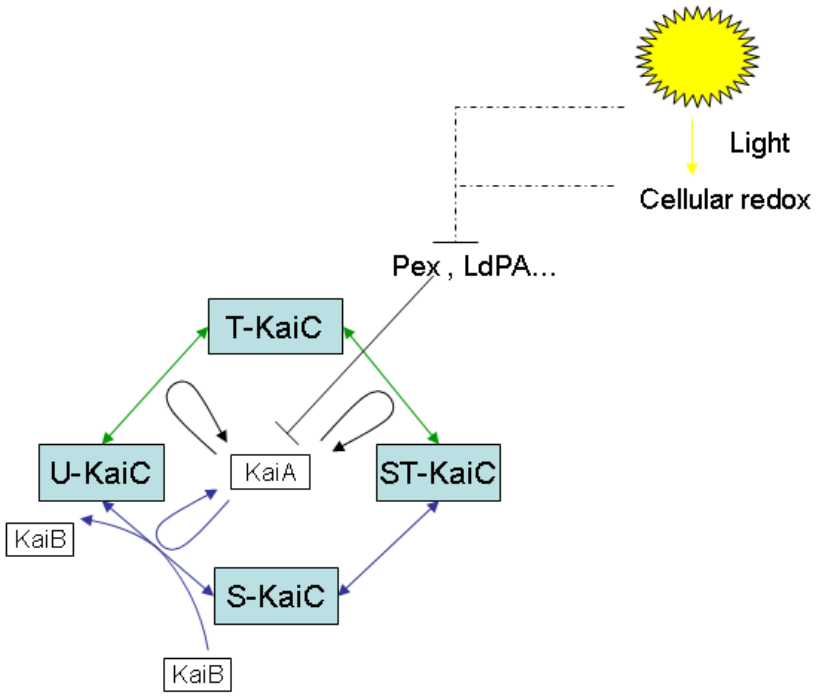

EUR 23772 EN - 2009

JRC EUROPEAN COMMISSION

ihcp Institute for Health and Consumer Protection

The mission of the IHCP is to provide scientific support to the development and implementation of EU policies related to health and consumer protection.

The IHCP carries out research to improve the understanding of potential health risks posed by chemical, physical and biological agents from various sources to which consumers are exposed.

European Commission
Joint Research Centre
Institute for Health and Consumer Protection

Contact information
Address: Via E. Fermi 2749, TP 272
E-mail: jose.zaldivar-comenges@jrc.it
Tel.: +39-0332-789202
Fax: +39-0332-785807

http://ihcp.jrc.ec.europa.eu/
http://www.jrc.ec.europa.eu/

Legal Notice
Neither the European Commission nor any person acting on behalf of the Commission is responsible for the use which might be made of this publication.

Europe Direct is a service to help you find answers to your questions about the European Union

Freephone number (*):

00 800 6 7 8 9 10 11

(*) Certain mobile telephone operators do not allow access to 00 800 numbers or these calls may be billed.

A great deal of additional information on the European Union is available on the Internet.
It can be accessed through the Europa server http://europa.eu/

JRC 50491

EUR 23772 EN
ISBN 978-92-79-11603-2
ISSN 1018-5593
DOI 10.2788/82036

Luxembourg: Office for Official Publications of the European Communities

© European Communities, 2009

Reproduction is authorised provided the source is acknowledged

Printed in Italy

Quality control insert

	Name	*Signature*	*Date*
Report Prepared by:	José-Manuel Zaldívar		16/02/09
Reviewed by: (Scientific level)	Eugenio Gutiérrez		18/02/09
Approved by: (Head of Unit)	Elke Anklam (ff)		02/03/09
Final approval: (IHCP Director)	Elke Anklam		02/03/09

CONTENTS

1. INTRODUCTION

Computational toxicology is defined (U.S. EPA, 2003) as "*the integration of modern computing and information technology with the technology of molecular biology and chemistry to improve risk assessment for toxic chemicals"*. Therefore, Computational toxicology should consider several computational disciplines including:

- Computational chemistry: physical-chemical modeling at the molecular level (quantum and molecular mechanics simulations) and chemo-informatics, e.g. QSAR.
- Computational Biology or Bioinformatics, which refers to development of molecular biology databases as well as processing, storage, distribution, analysis and interpretation.
- Systems biology: application of mathematical modeling and reasoning to the understanding of biological systems and the explanation of biological phenomena.

The objectives of Computational Toxicology are (U.S. EPA, 2003):

- to improve our understanding of the linkages between a chemical and its adverse effects from a continuum prospective, i.e. molecular to ecosystem level, see Fig. 1;
- to provide predictive models for chemical prioritization, screening and testing, able to reduce animal testing; and
- to provide quantitative risk assessment methodologies able to integrate human and ecological risk assessment.

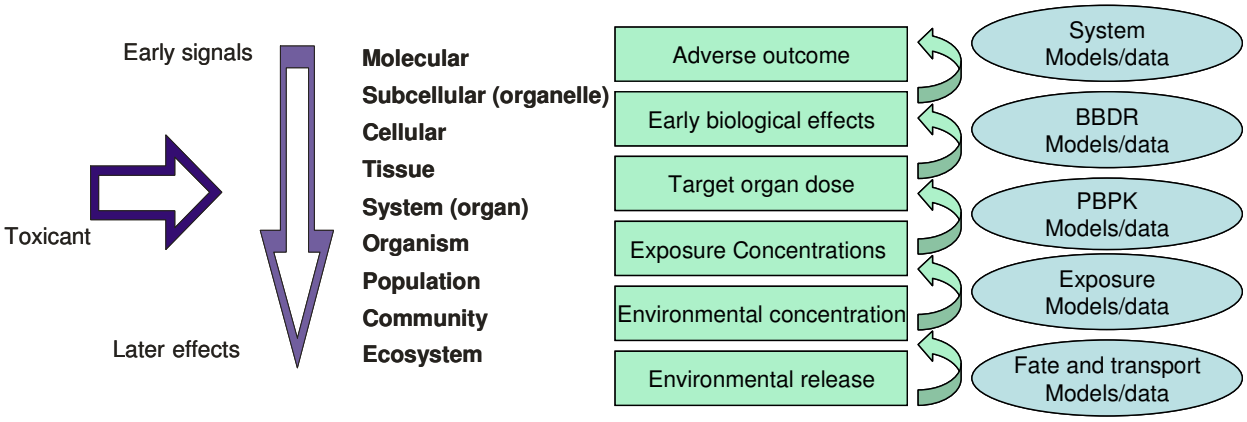

Figure 1. Sequential order of contaminant effects and cause-effect continuum and Computational Toxicology approaches (modified from van der Oost et al., 2003 and U.S. EPA, 2003). (Note: the term ecosystem is used in the broader sense, including humans; BBDR: Biology-based dose response; PBPK: Physiologically based pharmacokinetic).

Therefore, the final objective of Systems Toxicology is to be able to describe the response of a functioning organism to toxicants at all levels of biological organization and complexity by combining the information from several sources to gain a deeper understanding on the mechanisms of toxic action and by developing approaches allowing a more sensitive and earlier detection of adverse effects in

toxicity studies. This constitutes a big challenge since it requires to study interactions between genes, proteins and metabolites, and to integrate the results from different theoretical and experimental set-ups. However, a better understanding of the molecular mechanisms of toxicity may contribute to the extrapolation between experimental conditions, from low to high doses, from short term to chronic exposures, etc; thus, reducing the need for animal testing as well as the dose levels needed for toxicity elucidation. Systems Toxicology may be able to support *in vitro* experiments by discovering the underlying molecular mechanisms of toxicity better linking *in vitro* models to *in vivo* studies. Finally, Systems Toxicology may improve human health risk assessment, but it will require considerable standardization work, regulations and guidelines.

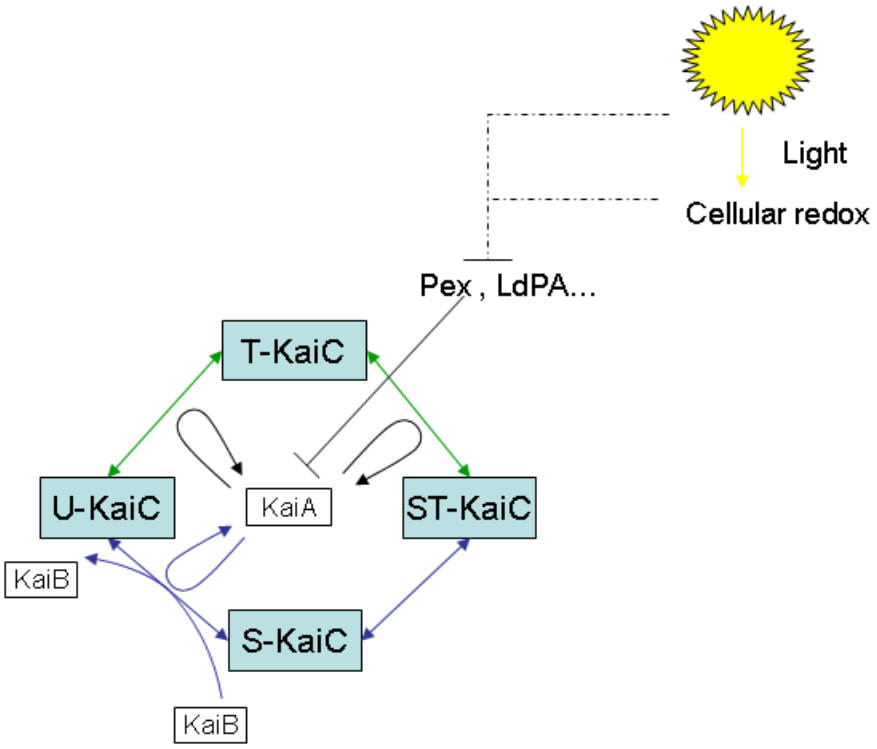

Figure 2. A model of KaiC phosphorilation oscillations with the role of KaiA and KaiB on the process and the effects of solar radiation (modified from Dong and Golden, 2008).

To analyze toxic effects from molecular level to population level, we have coupled a model of the circadian clock of cyanobacterium (Rust et al., 2007) with a bioenergetic growth model of phytoplankton (Dueri et al., 2009), see Fig. 2. Contaminants' effects are modelled by modifying the amount of proteins available in the circadian oscillator. This propagates in the ability of cyanobacteria to deal with solar radiation and their variation over a yearly cycle and subsequently in the growth of the population, assuming the the circadian oscillator is synchronized with the external light-dark cycles. Based on these assumptions, dose-response relationships have been also modelled.

2. METHODS AND APPROACH

2.1. CIRCADIAN OSCILLATION MODEL

Studies on the cyanobacterium *Synechoccus elongatus* have shown that it has an internal biological clock for measuring circadian time. Tomita et al. (2005) and Nakajima et al. (2005) showed that circadian oscillations in the cyanobacterium *Synechoccus elongatus* could be reproduced *in vitro* using three proteins: KaiA, KaiB and KaiC plus ATP. KaiA is a dimeric enzyme that enhances the autophosphorylation of KaiC, whereas KaiB antagonizes the activity of KaiA. KaiC (U-Kaic) is a hexameric enzyme that can phosphorylate and dephosphorylate at two positions: serine 431 (S-KaiC) and threonine 432 (T-KaiC, and on both ST-KaiC), see Fig. 2.

The model to simulate circadian oscillations was developed by Rust et al. (2007) and it was developed as an interlinked positive and negative feedback loop, see fig.2. Even though a simple negative loop is able to generate sustained oscillations, Tsai et al. (2008) demonstrated that to have a more robust system able to generate constant amplitude oscillations over a wide range of frequencies positive and negative loops were necessary. Following Rust et al. (2007), the model equations can be written as:

$$\frac{dT}{dt} = k_{UT} \cdot U + k_{DT} \cdot D - k_{TU} \cdot T - k_{TD} \cdot T \tag{1}$$

$$\frac{dD}{dt} = k_{TD} \cdot T + k_{SD} \cdot S - k_{DT} \cdot D - k_{DS} \cdot D \tag{2}$$

$$\frac{dS}{dt} = k_{US} \cdot U + k_{DS} \cdot D - k_{SU} \cdot S - k_{SD} \cdot S \tag{3}$$

where T, D and S denote T-KaiC, ST-KaiC and S-KaiC, respectively, and the rate constants k_{XY} are defined as:

$$k_{XY} = k_{XY}^{0} + \frac{k_{XY}^{A} \cdot A}{K_{1/2} + A} \tag{4}$$

with k_{XY}^{0} the rate constant when KaiA is not present and k_{XY}^{A} the influence of KaiA on this rate constant, i.e. positive promotion, negative inhibition; and A the active monomers of KaiA which are inhibited via S through KaiB, $A = \max\{0, [KaiA] - 2S\}$. The total concentration of KaiC can be expressed as:

$$[KaiC]_{total} = [U - KaiC] + [KaiC]_{p} = [U - KaiC] + [S - KaiC] + [T - KaiC] + [ST - KaiC] \tag{5}$$

The original values of the model obtained by Rust et al. (2007) are summarized in Table 1.

2.2. MODELLING THE EFFECTS OF CONTAMINANTS AT MOLECULAR LEVEL

To simplify the case study let us assume that there are three generic types of contaminants that

separately affect each protein, i.e. KaiA, KaiB and KaiC. Therefore the effects will be modeled by reducing the concentrations of KaiA and KaiC or by modifying the constant k_{DS}^{A} for the case of KaiB.

It is assumed that the contaminant interacts with each protein reducing their "effective" concentration in the organisms. There are several other possibilities to introduce contaminant effects such as the inhibition of S or T dephosphorylation, but a more detailed/realistic model would require experimental work on the real interactions as well as theoretical work to analyze the contaminant-docking site interactions.

Table 1. Parameters used in the model (Rust et al., 2007)

Parameter	Value	Units
k_{UT}^{0}	0	h^{-1}
k_{TD}^{0}	0	h^{-1}
k_{SD}^{0}	0	h^{-1}
k_{US}^{0}	0	h^{-1}
k_{TU}^{0}	0.21	h^{-1}
k_{DT}^{0}	0	h^{-1}
k_{DS}^{0}	0.31	h^{-1}
k_{SU}^{0}	0.11	h^{-1}
k_{UT}^{A}	0.479	h^{-1}
k_{TD}^{A}	0.213	h^{-1}
k_{SD}^{A}	0.506	h^{-1}
k_{US}^{A}	0.0532	h^{-1}
k_{TU}^{A}	0.0798	h^{-1}
k_{DT}^{A}	0.173	h^{-1}
k_{DS}^{A}	-0.319	h^{-1}
k_{SU}^{A}	-0.133	h^{-1}
$K_{1/2}$	0.43	μM

2.3. CYANOBACTERIA GROWTH MODEL

Let us assume a simple model without zooplankton grazing. Therefore, the variations of the phytoplankton, P (mmol N m^{-3}), is described in terms of *growth* (h^{-1}) and mortality m (h^{-1}),

$$\frac{dP}{dt} = growth_{Pd} \cdot P - m_{Pd} \cdot P \tag{6}$$

Phytoplankton growth is modelled as the product of the maximum specific growth rate μ_{max} multiplied with an overall limitation function, representing light limitation *f(I)*, temperature limitation *f(T)* and nutrient limitation $f(NO_3^-, NH_4^+)$, as:

$$growth_{Px} = \mu_{\max}^{Px} \cdot \min[f_1(I), f_2(T), f_3(NO_3^-, NH_4^+)] \tag{7}$$

The light limitation is parameterized according to Jassby and Platt (1976) by

$$f_1(I) = \tanh[a_p \cdot I(z,t)] \tag{8}$$

$$I(z,t) = I_s \cdot \exp[-(k_{water} + k_{phy}[Pf + Pd]) \cdot z] \tag{9}$$

where a_p (m^2 W^{-1})denotes the photosynthetic quantum efficiency parameter controlling the slope of *f(I)* versus the irradiance curve and I_s denotes the surface intensity of the PAR (photosynthetically active irradiance) taken as half of the incoming solar radiation. k_{water} (m^{-1}) is the extinction coefficient of the sea water and k_{phy} (m^2 mmol N^{-1}) is the phytoplankton self-shading coefficient.

The temperature limitation function for phytoplankton is based on Lancelot et al. (2002)

$$f_2(T) = \exp\left[-\left(\frac{T - T_{opt}}{T_{width}}\right)^2\right] \tag{10}$$

with T_{opt} and T_{width} being the optimal temperature in ºC and the range of suitable temperatures respectively.

The nutrient limitation is the sum of ammonium and nitrate limitation:

$$f_3(NO_3^-, NH_4^+) = f_a(NO_3^-) + f_b(NH_4^+) \tag{11}$$

where the limitations are expressed by the Michaelis-Menten uptake formulation:

$$f_a(NO_3^-) = \frac{[NO_3^-]}{K_{no} + [NO_3^-]} \cdot \exp(-\psi[NH_4^=]) \tag{12}$$

$$f_b(NH_4^+) = \frac{[NH_4^+]}{K_{nh} + [NH_4^+]} \tag{13}$$

where K_{no} and K_{nh} are half saturation constants (mmol N m^{-3}) for nitrate and ammonium uptake, respectively, and the exponent in Eq. (12) represents the inhibiting effect of ammonium concentration on nitrate uptake with ψ=3 m^3 mmol N^{-1} (Wrobleski, 1977).

The mortality of phytoplankton is expressed as a linear function of its biomass.

Table 2. Parameters used for the simulation of the phytoplankton model (Dueri et al., 2009).

Parameter	Definition	Value	Unit
a_p	Photosynthetis efficiency	0.01	m^2 W^{-1}
k_{water}	Light extinction coefficient in water	0.08	m^{-1}
k_{phy}	Phytoplankton self shading coefficient	0.07	mmol N^{-1}
μmax	Maximum growth rate	0.030	h^{-1}
$T_{opt,}$	Optimal temperature	15.0	ºC
T_{width}	Range of temperatures for cyanobacterium	7.0	ºC
K_{no}	Half saturation for nitrate uptake	0.5	mmol N m^{-3}
K_{nh}	Half saturation for ammonium uptake	0.2	mmol N m^{-3}
ψ	Ammonium inhibition parameter	3.0	m^3 mmol N^{-1}
m_P	mortality rate	0.0057	h^{-1}

In all the runs, the model is forced by imposing temperature and solar radiation sinusoidal forcing, which have the following form:

$$T = 9.76 \cdot \sin\left(2 \cdot \pi\left(\frac{t-114.74}{365}\right)\right) + 12.3 \quad (14)$$

$$I = 140.0 \cdot \left[\sin\left(2 \cdot \pi\left(\frac{t-120}{365}\right)\right) + 1\right] + 20.0 \quad (15)$$

These functions are typical of shallow systems in Europe. Furthermore, we have also included the duration of light during the year and the mean duration value using also two sinusoidal functions that gives the number of light minutes per day during the year (obtained also for European latitude).

$$L = 70.7 \cdot \sin\left(2 \cdot \pi\left(\frac{t-81.89}{365}\right)\right) + 729.1 \quad (16)$$

With L_h=L/60. The mean value for this duration, normally between 11.7 and 12.3 h is given by:

$$\mu_L = 0.15 \cdot \sin\left(2 \cdot \pi\left(\frac{t+3.12}{365}\right)\right) + 0.16 \cdot \sin\left(2 \cdot \pi\left(\frac{t+6.068}{182.5}\right)\right) + 0.02 \cdot \sin\left(2 \cdot \pi\left(\frac{t-3.21}{91.25}\right)\right) + 11.96 \quad (17)$$

Then I_s in Eq.(8) is calculated as:

$$I_s = I \cdot \exp\left[-\left(\frac{t_{day} - \mu_L}{0.5 \cdot L_h}\right)^2\right] \quad (18)$$

This produces a function that takes into account, when calculating the growth, the day and night cycles as well as their changing duration during the year.

An analysis of the variability of these functions on the effects of competition between phytoplankton, floating macroalgae and rooted macrophytes has been studied in Zaldívar et al. (2009) using a similar model, but it is outside the scope in this work to consider these aspects.

2.4. COUPLING CIRCADIAN CLOCK WITH THE GROWTH MODEL

According to the latest results by Dong and Golden (2008), it seems that *Synechoccus elongatus* clock senses the cellular redox state rather than the light intensity. However, the exact mechanism is not clear. What is know is that LdpA and CikA sense the cellular redox state and that both repress KaiA. In addition, Arita et al. (2007) and Kutsuna et al. (2007) have shown that Pex, a transcriptional repressor of KaiA, increases during the dark period having abundance sensitive to light, but the exact pathway is not clear. Furthermore, Smith and Williams (2006) have shown that KaiC is responsible for the slow compactation of *Synechoccus elongatus* chromosome during day and decompactation during night which seems to suggest that the circadian clock controls the global transcription rhythm by modifying the DNA topology.

Experiments by inactivation of the cikA (circadian input kinase) gene performed by Schmitz et al. (2000) have shown that the circadian period was shortened by two hours with changes in the phasing of several rhythms, and abolishes resetting of phase due to a pulse of several hours of darkness.

Let us formulate the following hypothesis: the correct functioning of *Synechoccus elongatus* requires that the organism synchronizes with the external light-dark conditions to optimize their growth and that this synchronization is carried out by a control mechanism that changes the KaiA concentration, between certain limits. Therefore, we will base our approach on the case of unidirectional coupling between two oscillators (Chen and Dong, 1998).

The hypothesis is in agreement with the origin of the internal biological clock that some prokaryotes posses for measuring daily time. According to Dong and Golden (2008), this constitutes an evolutive advantage for the organisms since they can anticipate and adjust for the dark-light effects in terms of temperature and light intensity rather that respond each time during the whole life cycle. In addition, spontaneous synchronization is a well-known characteristic of circadian oscillators in other species such as mammals (Gonze et al, 2005).

Therefore, we will assume that the concentration of KaiA can be expressed as:

$$[KaiA]_{total} = [KaiA]_i + k_{sync} \cdot \exp\left[-\left(\frac{t_{day} - \mu_L}{0.5 \cdot L_h} \right)^2 \right] \tag{19}$$

where $[KaiA]_i$ is the initial concentration of KaiA in the simulation, k_{sync} in the coupling strength coefficient and the light-dark cycle given by Eqs. (16)-(17).

To scale up the toxic effects from molecular level to population level, we will assume a baseline scenario and compare the differences with increasing doses of contaminants. We assume that for the correct functioning of the organism, external and internal clocks should be synchronized and the departure from this situation will, negatively, affect the growth of the organism. Therefore, we will measure the response, r_i, to a certain dose, d_i, as:

$$r_i = 1 - \frac{\sum_{i=1}^{365} \left([KaiC]_p - [KaiC]_p^{baseline} \right)^2}{\max(r_i)} \tag{20}$$

As before, this is an assumption that should be experimentally validated *in vivo* when the other hypothesis has been assessed *in vitro* or using molecular modelling approaches. In addition, the baseline scenario has been chosen as the one close to the modelling parameters used in the literature, but that it produces cycles of ~24 hours, i.e. $[KaiC]_{total}$=3.9 μM, [KaiA]= 1.26 μM; k_{DS}^A=-0.32 h^{-1} and k_{sync}=0.5 (however, the approach and methodology will not change if the baseline scenario is modified).

3. RESULTS AND DISCUSSION

3.1. UNSTRESSED AND STRESSED CIRCADIAN OSCILLATION MODEL

The numerical integration of the model given by Eqs. (1)-(4) using the parameters provided in Table 1 reproduces the circadian oscillation of KaiC phosphorylation, see Figs. 3-4. In Fig.3 the concentrations of the three phosphorylated species and the sum of all phosphorylated species are displayed versus time, whereas in Fig. 4 the state space is shown. As can be seen, the system converges to a limit cycle with a period of about 21 hours.

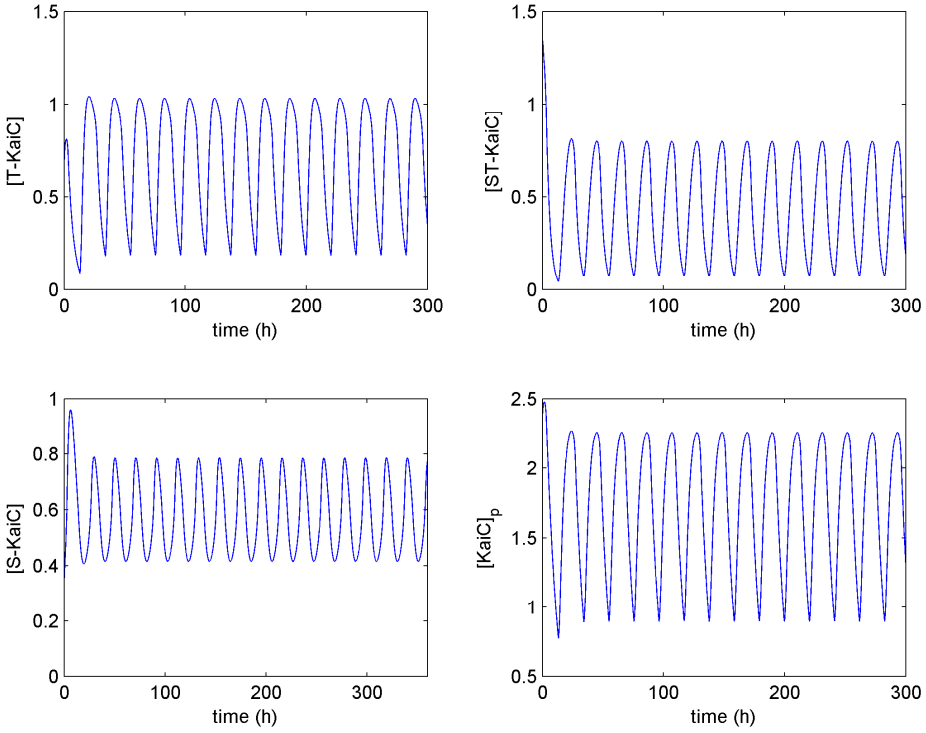

Figure 3. Simulation of the circadian oscillator with the parameters provided in Table 1 with initial conditions: [T-KaiC]= 20%$[KaiC]_{total}$; [ST-KaiC]= 40%$[KaiC]_{total}$; [S-KaiC]=;10%$[KaiC]_{total}$.

To analyze the effects of contaminants in the circadian oscillator we have changed, as discussed in Section 2, the concentrations of KaiA, the total concentration of KaiC and the constant k_{DS}^{A} related to the inhibition from KaiB on KaiA. The simulation results, in terms of oscillations amplitude and period are summarized in Figs. 5-6. As it can be observed, there exists a region in parameter space where there is a continuous change in the amplitude and period of the oscillations. In this region, the system converges to a limit cycle. However, for certain parameter's values, the oscillations stop and the system then converges to a fixed point. Between these two types of attractors there is a bifurcation point. To gain a better insight on the nonlinear dynamics of this system, a bifurcation analysis study, similar to the one carried out in Bacelar et al. (2009), is being conducted.

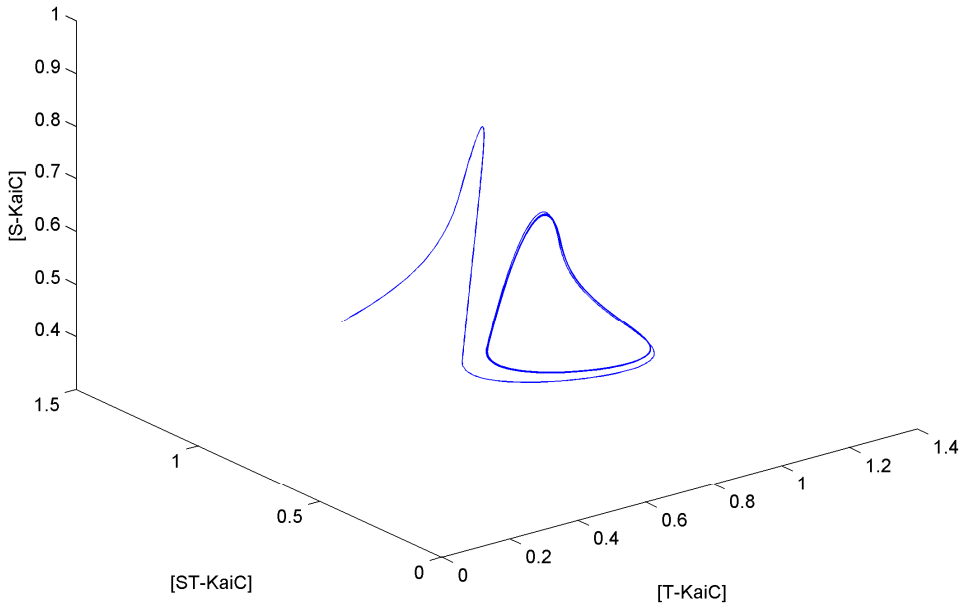

Figure 4. Limit cycle in the circadian oscillator. Parameters as in Table 1.

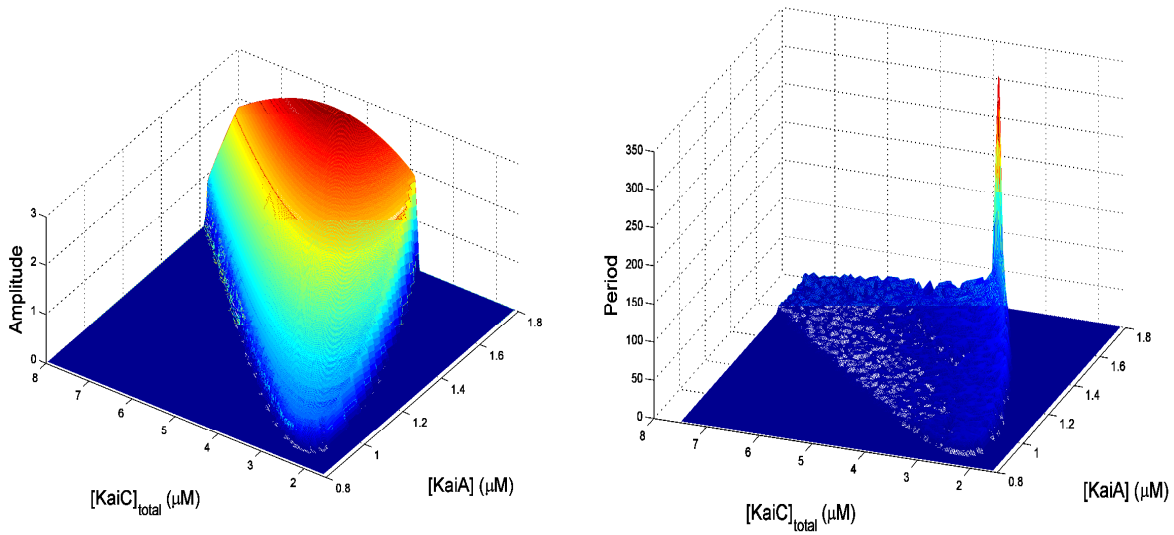

a/ b/

Figure 5.a/Amplitude and b/ period (hours, limit cycle) of the phosphorylated KaiC oscillations ($[KaiC]_p$=[T-KaiC]+[S-KaiC]+[ST-KaiC]) as a function of the total concentrations of KaiA and total concentration of KaiC.

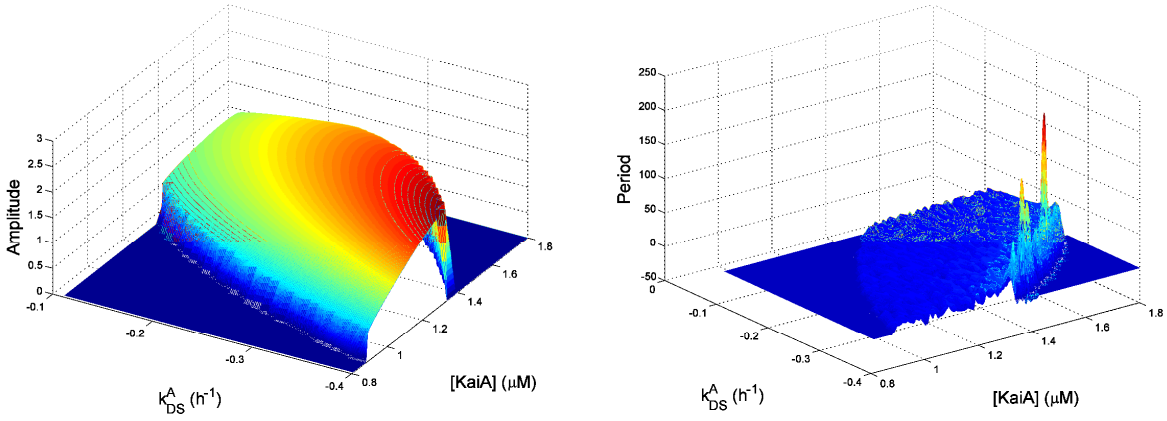

a/ b/

Figure 6. a/ Amplitude and b/ period (hours, limit cycle) of the phosphorylated KaiC oscillations ($[KaiC]_p$=[T-KaiC]+[S-KaiC]+[ST-KaiC]) as a function of the total concentrations of KaiA and k^A_{DS} which measures the effect of KaiB.

From this preliminary analysis we can conclude that the effects of contaminants able to interact with the three proteins that compose the system will change the amplitude and period of the circadian oscillator; being able, for certain values, to stop completely the oscillations. Of course, this is only a modelling hypothesis that should be confirmed with experiments and assumes that the model works properly outside of the domain in which was validated by Rust et al. (2007). However, similar effects – short circadian periods- have already been observed in vivo (Schmitz el al., 2000) by inactivation of the gene cikA (circadian input kinase)

Figures 7- 10 illustrate some particular cases of the dynamic behaviour of the circadian oscillator when [KaiA] is changed.

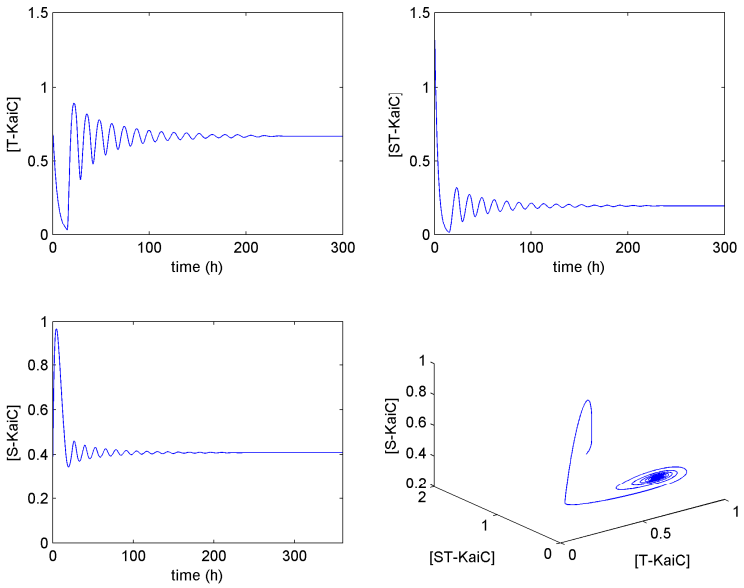

Figure 7. Simulation of the circadian oscillator with the parameters provided in Table 1, but with [KaiA]= 0.9 μM.

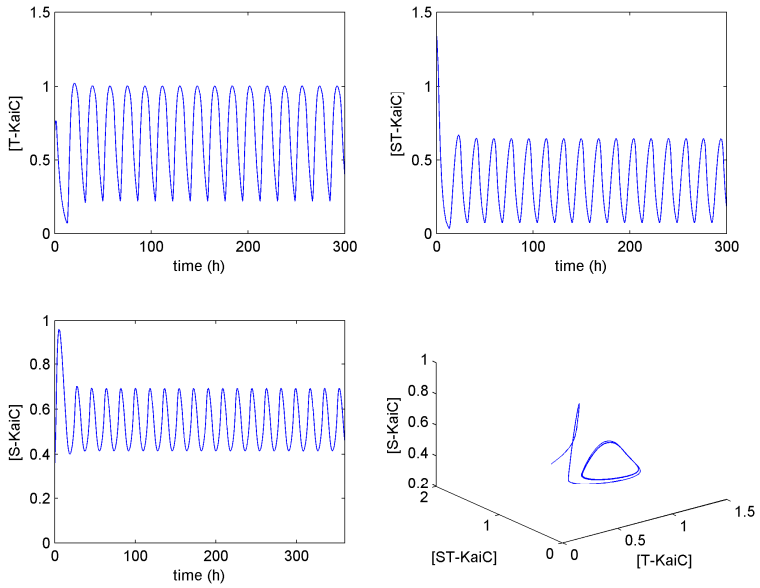

Figure 8. Simulation of the circadian oscillator with the parameters provided in Table 1, but with [KaiA]= 1.2 μM.

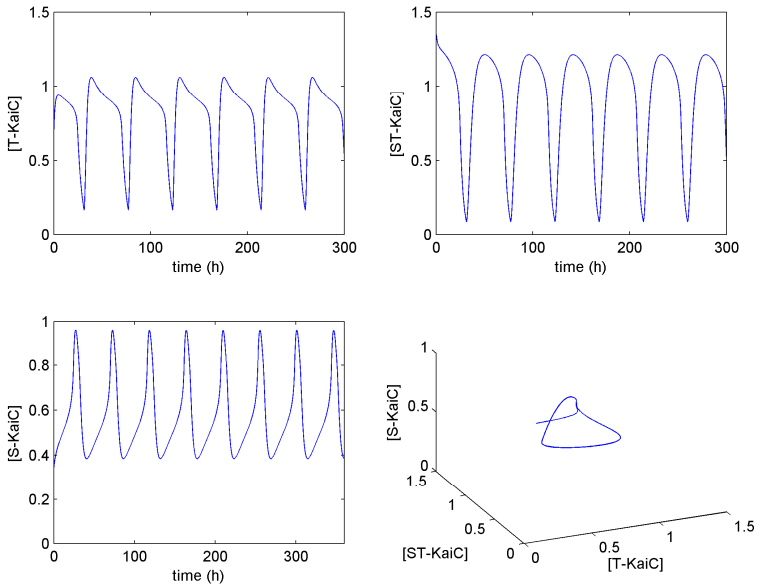

Figure 9. Simulation of the circadian oscillator with the parameters provided in Table 1, but with [KaiA]= 1.6 μM.

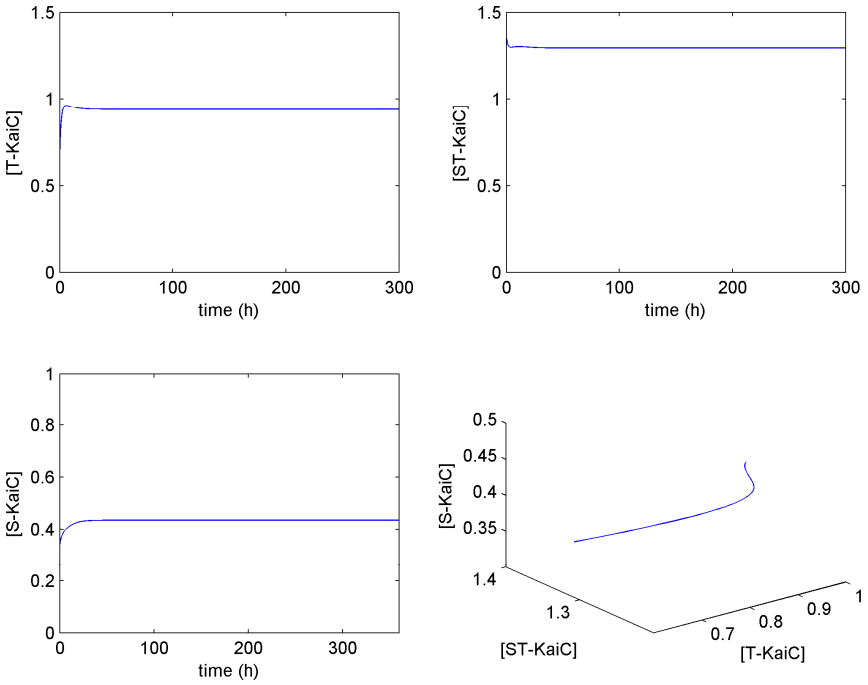

Figure 10. Simulation of the circadian oscillator with the parameters provided in Table 1, but with [KaiA]= 1.7 μM.

3.2. CYANOBACTERIA GROWTH MODEL

The cyanobacteria model was run under constant nutrient conditions using the temperature, light intensity, light-dark and duration, Eqs. (14)-(18), as forcing functions. An annual cycle of the cyanobacteria model is shown in Fig. 11a whereas a detail of the daily oscillations in phytoplankton mass due to the light-dark cycle are shown in Fig. 11b. The model results show the spring bloom biomass in spring and the decrease in autumn and winter. The shape of the curve is also typical of models where zooplankton grazing is not considered. In real situations, a phytoplankton bloom is followed by a zooplankton bloom that depletes phytoplankton biomass. The phytoplankton oscillations are in agreement with more detailed models that use meteorological data as forcing (Marinov et al., 2009). However, in that case, the oscillations are less evident since cloud coverage is also taken into account.

The fact that phytoplankton growth depends on light intensity and duration provides the coupling condition with the circadian oscillator model.

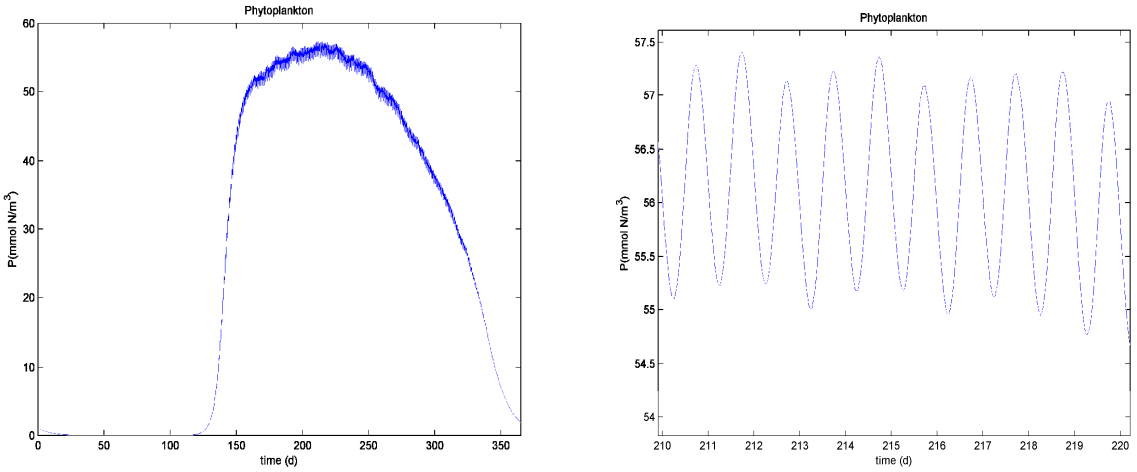

a/ b/

Figure 11.a/ One year simulation of phytoplankton growth with forcing conditions provided by Eqs. (14)-(18) and constant nutrient concentrations –[NO_3^-]= 0.8, [NH_4^+] = 0.3 mmol m^{-3}-; b/ detail from a/ showing the daily oscillations of phytoplankton biomass.

3.3. SYNCHRONIZATION OF THE COUPLED MODEL

As a first step, we introduced Eq. (19) in the circadian oscillator model and tested the values of k_{sync} assuming that during darkness the concentration of KaiA decreases, i.e. k_{sync}>0 (Kutsuna et al., 2007). Depending on the coupling strength the system synchronizes to the light-dark oscillations. Figure 12 shows an example of one year simulation of the circadian oscillator when coupling is acting. It is also possible to observe the annual modulation of [ST-KaiC] and [S-KaiC] in the daily oscillations. In this case the system dynamics in phase space is not a limit cycle but changes as the light-dark conditions change, see Fig. 13. The coupling takes place approximately after the first eighteen days, Fig 14a; examples of the coupling at two different periods during the year are shown in Figs.14b and 14c. Similar behaviour can be observed with different initial parameters and coupling strengths, but several types of synchronization behaviour may occur. For example, Fig. 15 shows a 48 h synchronization for *ksync*=0.1 and $[KaiC]_{total}$=3.9 and [KaiA]=1.26 μM, respectively. A detailed analysis of synchronization mechanisms is outside the scope of this theoretical work, since it would require *in vivo* experiments and a metabolomic approach to measure the change in concentrations of several compounds responsible for the functioning of the system.

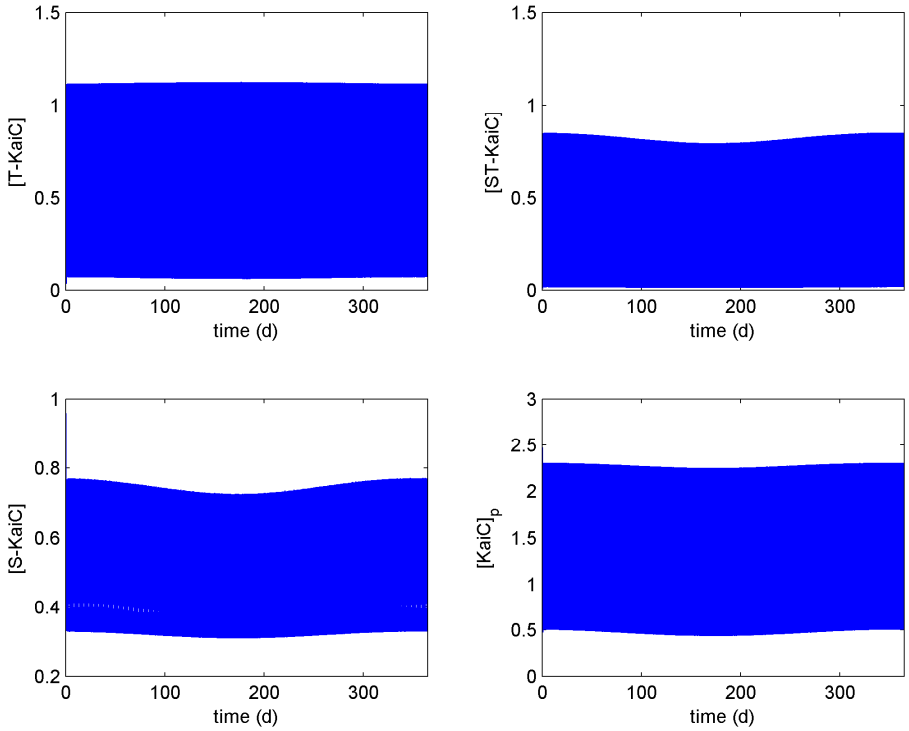

Figure 12. One year simulation of the forced circadian oscillator with the parameters provided in Table 1 with and k_{sync}=1.

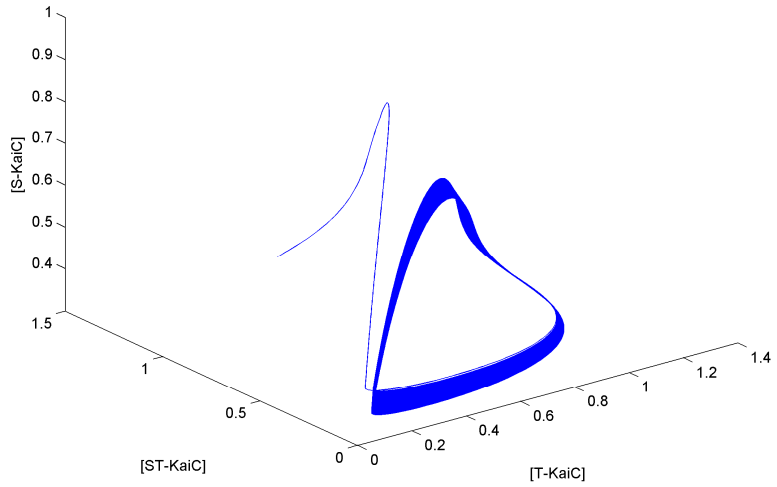

Figure 13. State-space representation of the circadian oscillator when forced with dark-light conditions during one year, k_{sync}=1.

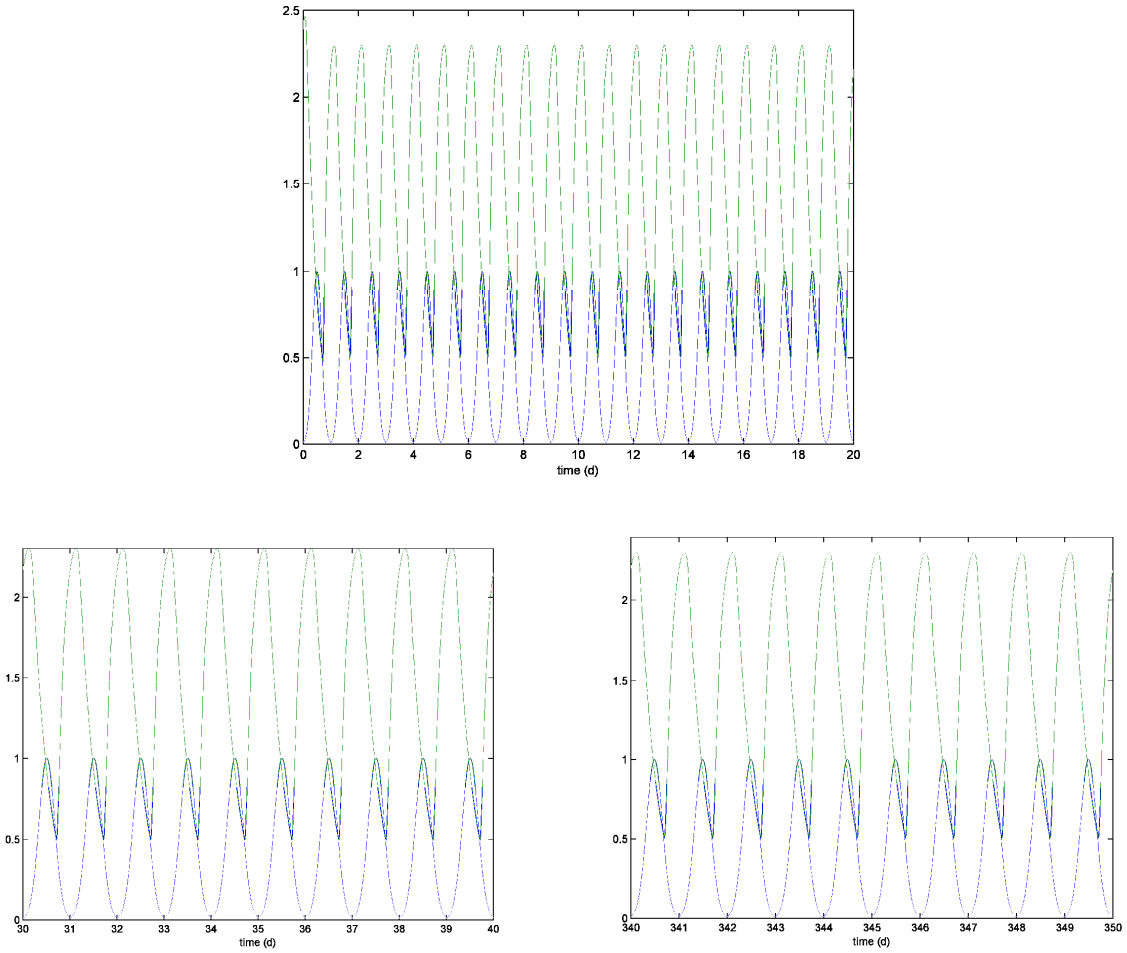

Figure 14. Simulated phosphorylated KaiC concentration, $[KaiC]_p$=[S-KaiC]+[T-KaiC]+[ST-KaiC] -green line- and light-dark cycles for two periods of the year – blue line-. Parameters: $[KaiC]_{total}$=3.4 μM, [KaiA]=1.3 μM and k_{sync}=1.

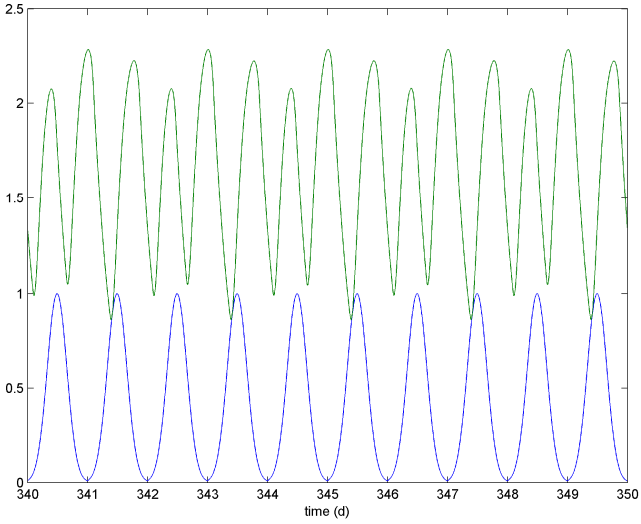

Figure 15. Simulated phosphorylated KaiC concentration, $[KaiC]_p$=[S-KaiC]+[T-KaiC]+[ST-KaiC] -green line- and light-dark cycles at the end of the year- blue line-, notice the 48h synchronization period. Parameters: $[KaiC]_{total}$=3.9 μM, [KaiA]=1.26 μM and k_{sync}=0.1.

3.4. SIMULATED DOSE-RESPONSE CURVES IN THE COUPLED MODEL

As discussed above, let us analyze the case of three contaminants that interact separately with the three proteins, KaiC, KaiA, KaiB, that form the circadian oscillator. Therefore we will measure the dose as the decrease of the amount of concentration with respect to our baseline, and the effect as the normalized distance from the baseline, represented by the oscillations in concentration of the phophorylated KaiC compounds, during one year. In this example, the baseline scenario has been defined as (see Section 2.4): $[KaiC]_{total}$=3.9 μM, [KaiA]= 1.26 μM; and k_{DS}^{A} =-0.32 h^{-1}; k_{sync}=0.5.

Figures 16-18 represent the dose-response curve for three hypothetic contaminants that interact with the three proteins. Strikingly, the shape of the curves is quite similar to those obtained experimentally. In addition, even though all contaminants interact with the circadian oscillator, the shape of the dose-response curves is also different depending on the mode of interaction. Similar results should be also hypothesized for other molecular machinery and, therefore, this seems a plausible explanation for the fact that different chemical compounds can act of the same system even if there are no structural similarities between them.

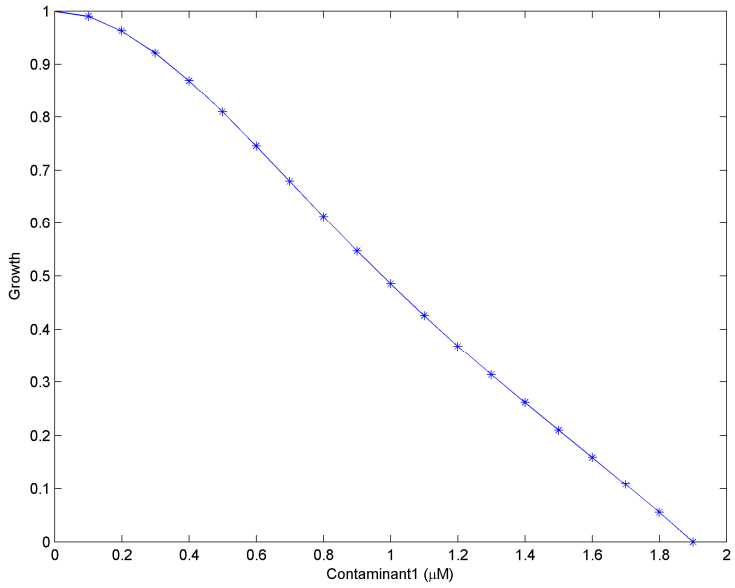

Figure 16. Simulated dose-response curve for a contaminant that interacts with $[KaiC]_{total}$.

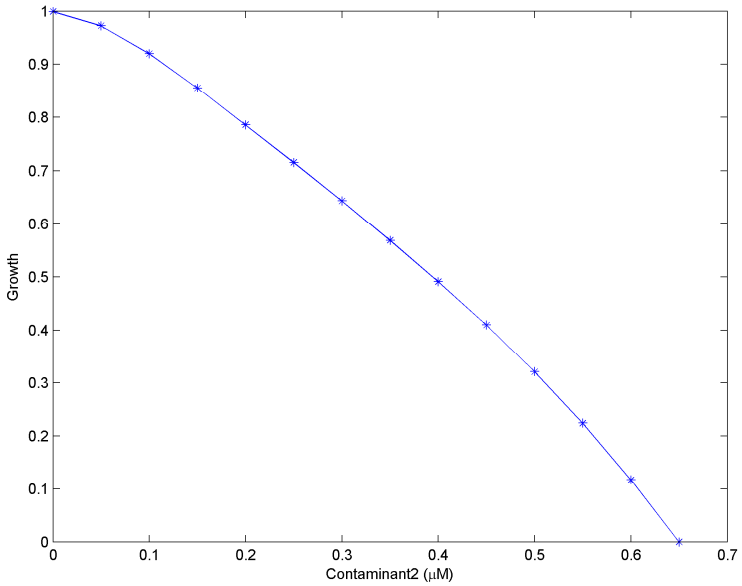

Figure 17. Simulated dose-response curve for a contaminant that interacts with [KaiA].

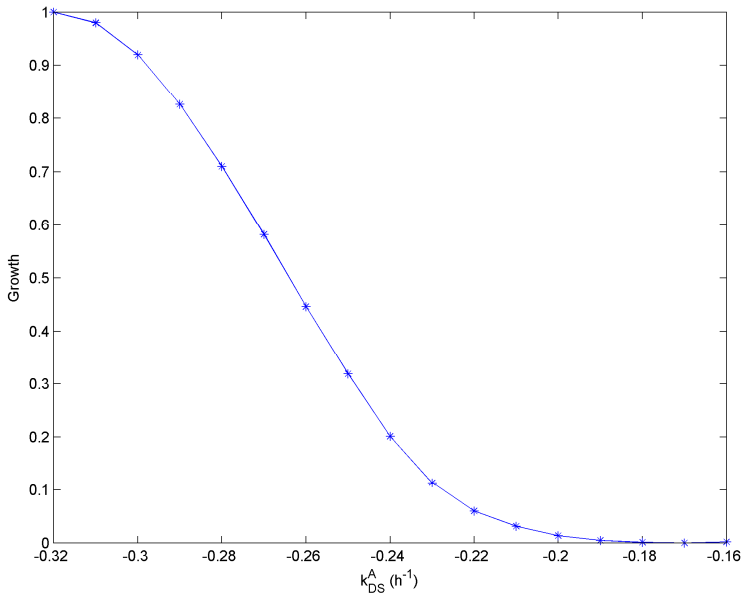

Figure 18. Simulated dose-response curve for a contaminant that interacts with [KaiB] through k_{DS}^{A}.

Finally, as an example, Fig. 19 shows the dynamics of the cyanobacteria population exposed to constant doses of a contaminant that reduces its growth by 10, 20, 30 and 40% after the first year, respectively. The figure also illustrates the propagation of the effects from individual level to population level, the chronic effects of exposure and the response time of the system.

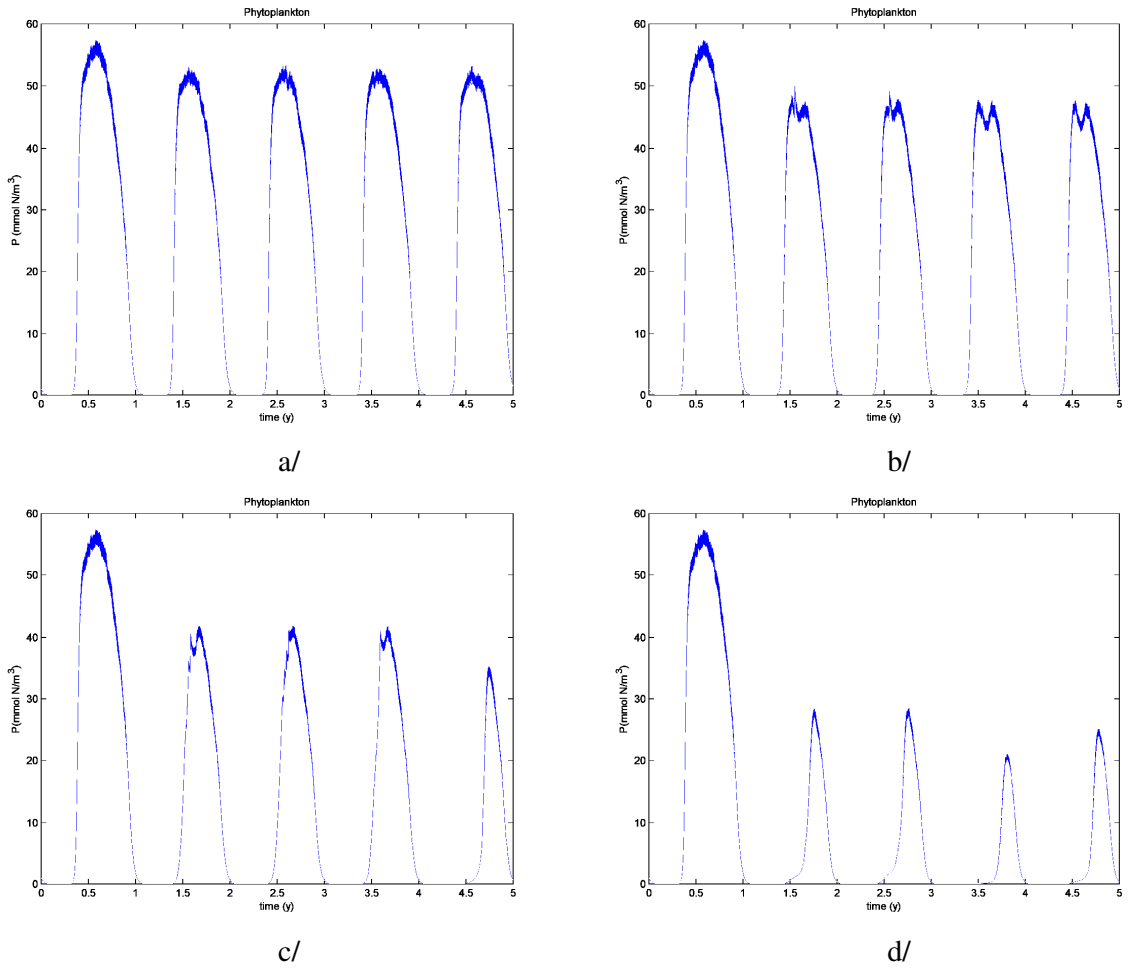

Figure 19. Simulated cyanobacteria model with a constant contaminant dose that reduces by a/ 10%; b/20%; c/30%; d/40% the growth after the first year.

4. CONCLUSIONS

A first attempt to analyze the possible toxic effects of several compounds, acting at molecular level, on the population lhas been carried out using a coupled modelling approach based on a circadian oscillators and a cyanobacteria growth model. To develop further this approach, several assumptions have been made on the linkage between the circadian clock functioning and the population growth as well as on the effects of contaminants at molecular level. Synchronization with light-dark conditions has been introduced as the coupling mechanism and its los as the influencing mechanism in the growth model. Then dose-response curves have been developed. The obtained curves show a striking resemblance to those obtained experimentally, even though no assumptions have been made in the model about their shape.

The modelling results suggest new experimental approaches to validate the assumptions as well as to understand toxicity effects, the functioning and malfunctioning of molecular machinery and possible consequences. In addition, several modelling hypothesis could be refined when experimental data become available.

The results point to the need that to understand toxic effects we have to focus our study on the interactions that a certain compound may have with proteins, and/or DNA, since the result of these interactions will determine the final mode of action at macroscopic level. Therefore an intermediate step for assessing toxic effects, based on the type of interaction at molecular level, is proposed for developing a coherent toxicity framework analysis. This would explain why completely different compounds have the same mode of actions whereas similar ones at the level of structure have sometimes different mode of action.

Since the molecular clock system is quite simple, experiments could be carried out *in vitro* to validate the model results as well as the concentration thresholds. In addition, the structures of the proteins KaiA, KaiB and KaiC are known, so it could be possible, in principle, to select the chemicals that dock (block the functioning) of one but not the others proteins, to compare experimental and modelling results. Finally, *in vivo* experiments with *Synechoccus elongatus* could be performed.

Missing aspects in the model include the possible delays due to the kinetics of the proteing-ligand (contaminant) docking and due to the diffusion of the contaminant from the water to the organism, to take into account internal concentrations.

5. REFERENCES

Arita, K., Hashimoto, H., Igari, K., Akaboshi, M., Kutsuna, S., Sato, M., Shimizu, T., 2007. Structural and biochemical characterization of a cyanobacterium circadian clock-modifier protein, The Journal of biological chemistry 282, 1128-1135.

Bacelar, F. S., Dueri, S., Hernández-García, E. and Zaldívar, J.M., 2009. Joint effects of nutrients and contaminants on the dynamics of a food chain in marine ecosystems. Mathematical Biosciences 218, 24-32.

Chen, G., Dong, X. 1998 *From chaos to order: Methodologies, perspectives and applications*. World Scientific, Singapore.

Dong, G., Golden, S.S., 2008. How a cyanobacterium tells time. Current Opinion in Microbiology 11, 541-546.

Dueri, S., Hjorth, M., Marinov, D., Dallhof, I. and Zaldívar, J.M., 2009. Modelling the combined effects of nutrients and pyrene on the plankton population: Validation using mesocosm experimental data and scenario analysis. Ecological Modelling (accepted)

Gonze, D., Bernard, S., Waltermann, C., Kramer, A., Herzel, H., 2005. Spontaneous synchronization of coupled circadian oscillators. Biophysical Journal 89, 120-129.

Jassby, A. D., Platt, T., 1976. Mathematical formulation of the relationship between photosynthesis and light for phytoplankton. Limnology and Oceanography 21, 540-547.

Kutsuna, S., Kondo, T., Ikegami, H., Uzumaki, T., Katayama, M., Ishiura, M., 2007. The cricadian clock-related gene pex regulates a negative cis element in the kaiA promoter region. Journal of Bacteriology 189, 7690-7696.

Lancelot, C., J. Staneva, D. Van Eeckhout, J.M. Beckers, Stanev, E., 2002. Modelling the Danube-influenced north-western continental shelf of the Black Sea. II. Ecosystem response to changes in nutrient delivery by the Danube river after its damming in 1972. Estuarine and Coastal Shelf Science 54, 473-499.

Marinov, D. Dueri, S., Puillat, I., Carafa, R., Jurado, E., Berrojalbiz, N. Dachs, J. and Zaldívar, J.M., 2008. Integrated modeling of Polycyclic Aromatic Hydrocarbons (PAHs) in the marine ecosystem: Coupling of hydrodynamic, fate and transport, bioaccumulation and planktonic food web models. Marine Pollution Bulletin (submitted).

Nakajima M., Imai, K., Ito, H., Nishiwaki, T., Murayama, Y., Iwasaki, H., Oyama, T., Kondo, T., 2005. Reconstruction of circadian oscillation of cyanobacterial KaiC phosphorylation in vitro. Science 308, 414-415.

Rust, M. J., Markson, J. S., Lane, W. S., Fisher, D. S., O'Shea, E. K., 2007. Ordered phosphorylation governs oscillation of a three-protein circadian clock. Science 318, 809-812.

Schmitz, O., Katayama, M., Williams, S.B., Kondo, T., Golden, S.S. 2000. CikA, a bacteriophytochrome that resets the cyanobacterial circadian clock. Science 289, 765-768.

Smith R.M., Williams S.B., 2006. Circadian rhythms in gene transcription imparted by chromosome compactation in the cyanobacterium Synechococcus elongates. Proceedings of the National Academy of Sciences USA 103, 8564-8569.

Tomita, J., Nakajima, M., Kondo, T., Iwasaki, H., 2005.No transcription-translation feedback in circadian rhythm of KaiC phosphorylation. Science 307, 251-254.

Tsai, T. Y-C., Choi, Y. S., Ma, W., Pomerening, J.R., Tang, C., Ferrell Jr., J. E., 2008. Robust, tunable biological oscillations from inerlinked positive and negative feedback loops. Science 321, 126-129.

U.S. EPA, 2003. A framework for a computational toxicology research program. Washington D.C. EPA600/R-03/65.

Van der Oost, T., Beyer, J. and Vermeulen, N. P. E., 2003. Fish bioaccumulation and biomarkers in environmental risk assessment: a review. Environmental Toxicology and Pharmacology 13, 57-149.

Wroblewski, J.A., 1977. A model of phytoplankton bloom formation during variable Oregon upwelling. Journal of Marine Research 35, 357-394.

Zaldívar, J.M., Bacelar, F., Dueri, S. Marinov, D. Viaroli, P., Hernandez, E., 2009. A modeling approach to nutrient and temperature driven regime shifts in shallow coastal ecosystems: Competition between seagrass and macroalgae. Ecological Modelling (in press, 0.1016/j.ecolmodel.2009.01.022).

European Commission

EUR 23772 EN – Joint Research Centre – Institute for Health and Consumer Protection
Title: Analysis of toxicity effects from molecular to population level: Circadian oscillator case study
Author(s): José-Manuel Zaldívar
Luxembourg: Office for Official Publications of the European Communities
2008 – 24 pp. – 21 x 29,7 cm
EUR – Scientific and Technical Research series – ISSN 1018-5593
ISBN 978-92-79-11603-2
DOI 10.2788/82036

Abstract To analyze how toxic effects propagate from molecular to population level, a simple model of a circadian oscillator has been coupled with a cyanobacteria growth model. It has been assumed that the circadian oscillator synchronizes with light-dark environmental conditions and toxicants affect this synchronization reducing the population growth. Then dose-response curves have been developed. The results evidence that to understand toxic effects we have to focus our study on the interactions that a certain compound may have with proteins, and/or DNA, since the result of these interactions will determine the final mode of action at macroscopic level. Therefore an intermediate step for assessing toxic effects has been proposed.

How to obtain EU publications

Our priced publications are available from EU Bookshop (http://bookshop.europa.eu), where you can place an order with the sales agent of your choice.

The Publications Office has a worldwide network of sales agents. You can obtain their contact details by sending a fax to (352) 29 29-42758.

The mission of the JRC is to provide customer-driven scientific and technical support for the conception, development, implementation and monitoring of EU policies. As a service of the European Commission, the JRC functions as a reference centre of science and technology for the Union. Close to the policy-making process, it serves the common interest of the Member States, while being independent of special interests, whether private or national.

LB-NA-23772-EN-C

ISBN 978-92-79-11603-2